Long non-coding RNA ABHD11-AS1 inhibits colorectal cancer progression through interacting with EGFR to suppress the EGFR/ERK signaling pathway

SHIMING TAN[1,2*], SHIZHEN LI[1,2*], LONGZHENG XIA[1,2], XIANJIE JIANG[1,2], ZONGYAO REN[1,2], QIU PENG[1,2], MINGJING PENG[1,2], WENJUAN YANG[1], XUEMENG XU[1,2], LINDA OYANG[1,2], MENGZHOU SHEN[1,2], JIEWEN WANG[1,2], HAOFAN LI[1], NAYIYUAN WU[1,2], YANYAN TANG[1,2], QIANJIN LIAO[3], JINGUAN LIN[1,2] and YUJUAN ZHOU[1,2]

[1]The Affiliated Cancer Hospital of Xiangya School of Medicine, Central South University/Hunan Cancer Hospital, Hunan Key Laboratory of Cancer Metabolism, Changsha, Hunan 410013, P.R. China; [2]Hunan Engineering Research Center of Tumor Organoid Technology and Application, Public Service Platform of Tumor Organoid Technology, Changsha, Hunan 410013, P.R. China; [3]Department of Oncology, Hunan Provincial People's Hospital (The First Affiliated Hospital of Hunan Normal University), Changsha, Hunan 410005, P.R. China

Received September 5, 2024; Accepted January 15, 2025

DOI: 10.3892/ijo.2025.5726

Abstract. Long non-coding (lnc)RNAs participate in colorectal cancer (CRC) occurrence and progression. The present study aimed to investigate whether lncRNA ABHD11-AS1 regulates malignant biological behavior of CRC cells. Bioinformatic analysis, reverse transcription-quantitative PCR and *in situ* hybridization revealed that ABHD11-AS1 expression was decreased in CRC samples and associated with an unfavorable prognosis. ABHD11-AS1 overexpression significantly decreased proliferation, migration and invasion of CRC cells, whereas ABHD11-AS1 inhibition had the opposite effects. ABHD11-AS1 interacted with EGFR to inhibit EGFR phosphorylation and attenuate EGFR/ERK signaling, which in turn suppressed the malignant biological behavior of CRC cells. The tumor suppressor function of ABHD11-AS1 was attenuated by the EGFR agonist NSC228155. Finally, resveratrol (RSV) inhibited CRC cell proliferation, migration and invasion, which may be associated with RSV-induced decrease in SPT6 homolog, histone chaperone and transcription elongation factor protein expression and increase in ABHD11-AS1 transcript levels. ABHD11-AS1 inhibited the phosphorylation of EGFR and decreased EGFR/ERK signaling by interacting with EGFR, thereby delaying the progression of CRC. The ABHD11-AS1/EGFR/ERK axis may be a novel therapeutic target for preventing CRC progression.

Correspondence to: Professor Yujuan Zhou or Professor Jinguan Lin, The Affiliated Cancer Hospital of Xiangya School of Medicine, Central South University/Hunan Cancer Hospital, Hunan Key Laboratory of Cancer Metabolism, 283 Tongzipo Road, Changsha, Hunan 410013, P.R. China
E-mail: yujany_zhou@163.com
E-mail: linjinguan11@sina.com

*Contributed equally

Key words: ABHD11-AS1, EGFR, resveratrol, SPT6, colorectal cancer

Introduction

Colorectal cancer (CRC) is one of the most common malignant tumors of the digestive system in China, with new cases (517,100) and deaths (240,000) rank among the top five of all types of cancer and show an increasing trend in 2022 (1,2). Revealing the molecular mechanisms underlying CRC development is important for increasing the effectiveness of CRC treatment and improving the prognosis.

Long non-coding RNAs (lncRNAs) are RNA transcripts that >200 nucleotides in length that have notable spatiotemporal and temporal expression specificity and are widely involved in gene regulation (3). Previous studies have shown that lncRNAs regulate CRC progression. For example, the lncRNA PVT1 promotes CRC proliferation and metastasis via the microRNA (miR)-24-3p/neuropilin 1 axis (4) and LINC00955 acts as a molecular scaffold for tripartite motif containing 25 and Sp1 transcription factor, leading to G0/G1 cell cycle arrest in CRC cells (5). In addition, lncRNAs constitute a potential class of biomarkers for CRC screening, diagnosis and prognosis. Glycolysis- and necrosis-associated lncRNAs are used for clinical prognostic evaluation (6,7). lncRNAs play important roles in CRC progression.

lncRNAs have many functions in cancer. lncRNAs may play contradictory roles by activating different signaling pathways. For example, lncRNA H19 acts as an oncogene that activates epithelial-mesenchymal transition (EMT) to promote proliferation, migration and invasion of skin squamous cell carcinoma cells (8). However, lncRNA H19 can inhibit osteosarcoma by regulating the expression of small nucleolar RNA SNORA7A (9). High levels of lncRNA ABHD11-AS1 expression in pancreatic cancer (PC) tissue are associated with

distant metastasis, TNM stage and tumor differentiation (10). However, another study revealed that ABHD11-AS1 expression is downregulated in patients with PC with positive lymphatic metastasis (11). These findings reflect the heterogeneity of lncRNAs.

The aim of the present study was to investigate the role and mechanism of lncRNA ABHD11-AS1 in CRC to reveal how ABHD11-AS1 regulates CRC cell proliferation, migration, and invasion through interaction with EGFR, and to explore the regulatory effect of resveratrol on ABHD11-AS1 transcription, with the goal of evaluating its potential in CRC treatment.

Materials and methods

Human tissue samples. All the participants signed informed consent (approval no. KYJJ-2022-240). The inclusion criteria were as follows: i) Patients who were confirmed to have CRC by post-operative pathological analysis; ii) medical records were complete. The exclusion criterion were patients with two or more concurrent primary malignancies. The study was approved by the Ethical Review Committee of Hunan Cancer Hospital. A total of 66 surgical specimens (39 males and 27 females; median age, 66.5 years and an age range of 27-82 years) and their adjacent non-tumor (≥5 cm distal to tumor margins) samples (n=39) from patients with CRC at Hunan Cancer Hospital, Changsha, China, between June 2007 and September 2011 were collected, fixed (10% neutral buffered formalin and fix for 24 h at room temperature.) and paraffin-embedded.

Cell lines and culture. The human normal colon epithelial cell line NCM460 (cat. no. CL0393) and four colon cancer cell lines, HCT116 (cat. no. CL0125), HT29 (cat. no. CL0163), SW480 (cat. no. CL0303) and SW620 (cat. no. CL0305), were obtained from Hunan Fenghui Biotechnology. All cells were identified by STR. The culture conditions were as previously described (12). NCM460 and HCT116 cells were cultured in DMEM (Gibco; Thermo Fisher Scientific, Inc.) supplemented with 10% FBS (ZETA LIFE, Inc.). HT29, SW480 and SW620 cells were cultured in RPMI-1640 (Gibco; Thermo Fisher Scientific, Inc.) supplemented with 10% FBS. ABHD11-AS1 overexpression plasmid and three ABHD11-AS1 short hairpin (sh)RNAs (sh-ABHD11-AS1-1, sh-ABHD11-AS1-2 and sh-ABHD11-AS1-3) were obtained from Shanghai GeneChem Co., Ltd. (Table SI). HCT116 and SW620 cells were transfected with 2 μg plasmid (ABHD11-AS1: GV658 vector, pcDNA3.1-CMV-3flag-EF1A-zsGreen-sv40-puromycin; the negative vector: GV658 vector, pcDNA3.1; shRNA: GV102 vector; the negative control sequence was 5'-TTCTCCGAACGTGTCACGT-3'.) (Shanghai GeneChem Co., Ltd.) using Lipofectamine 3000 (Invitrogen; Thermo Fisher Scientific, Inc.) at room temperature for 6-8 h before changing the medium. The subsequent experiments were carried out 48 h after transfection. The effects of overexpression and knockdown were detected by quantitative (q)PCR.

CCK-8 assay. CCK-8 assay were performed as described previously (13). Briefly, cell proliferation was assessed using the Cell Counting Kit (ZETA LIFE, Inc.; cat. no. K009-500) in accordance with the manufacturer's protocol. Cells in the logarithmic growth phase) was seeded in quintuplicate at a density of 5,000 cells per well onto 96-well plates with 100 μl of medium per well and cultured in humidified air with 5% CO_2 at 37˚C. Complete medium containing 10% CCK-8 reagent was added at time points of 0, 24, 48, and 72 h, respectively, and the OD value was detected at 450 nm after continued incubation for 2 h. The proliferation curves were plotted using Prism 8.0 software.

Colony formation assay. Colony formation assays were performed as described previously (13). Briefly, transfected cells (2,000 cells/dish) were seeded onto 6 cm dishes and incubated in humidified air with 5% CO_2 at 37˚C for 2 weeks, then stained with 0.1% crystal violet. Images of visible colonies were captured using a FUSION SOLO S (VILBER), and colonies containing >50 cells were counted and quantified using ImageJ software.

Drug treatment. The working concentrations of resveratrol (RSV) (cat. no. SC0276-10 mM, Beyotime Biotechnology, Jiangsu, China) were as we measured the IC50 values. In brief, after treatment with RSV the cells were incubated in humidified air with 5% CO_2 at 37˚C for 48 h and used for subsequent experiments. For NSC228155 (cat. no. S8312, Selleck, Inc.), an EGFR activator, cells were treated with 100 μM NSC228155 in humidified air with 5% CO_2 at 37˚C for 12 h and then used for subsequent experiments. For chrysophanol (cat. no. S2406, Selleck, Inc.), an EGFR inhibitor, cells were treated with 10 μM chrysophanol in humidified air with 5% CO_2 at 37˚C for 48 h and then used for subsequent experiments.

Immunofluorescence. Cells seeded in crawls were fixed with 4% paraformaldehyde for 15 min, followed by blocking with 5% BSA for 1 h, and then incubated with anti-EGFR antibody (1:50, A11577, ABclonal) at 4˚C overnight, after three washes with 0.5 M PBS, cells were incubated with appropriate fluorescent secondary antibodies for 1 h at 37˚C. The nucleus was stained with 10 μM DAPI (cat. no. AI-50, ZETA LIFE, Inc.) for 10 min at room temperature and cells were photographed under a confocal microscope (Carl Zeiss AG, Germany).

Transwell migration and invasion and wound healing assays. The pore size of the Transwell plates was 8 μm (cat. no. 3422, Costar, Inc.). A total of 200 μl RPMI-1640 medium containing transfected cells ($2x10^4$ cells/well) was added to the upper chambers and 600 μl RPMI-1640 medium containing 20% FBS was added to the lower chambers. For the invasion assay, Matrigel was used to coat the upper chambers for 30 min at 37˚C (50 μl/well, cat. no. 356230, BD Pharmingen; BD Biosciences). After incubation for 48 h in humidified air with 5% CO_2 at 37˚C, the invading cells were fixed with 4% paraformaldehyde at room temperature for 20 min and removed from the upper chamber. Fixed cells were stained with 0.1% crystal violet for 15 min at room temperature. Images of the crystal violet-stained cells were captured and the cells were counted using a light microscope.

For wound healing assay, HCT116 and SW620 cells were inoculated into 6-well plates. When cells reached 90-95% confluence, the monolayer was scraped with a sterile 10 μl pipette tip and dislodged cells were removed with PBS. The cells were cultured in serum-free medium at 37˚C for 48 h,

and images were acquired using a Zeiss light microscope. The wound area at the same location was subsequently measured by ImageJ (V1.54d, National Institutes of Health). The cell migration rate was calculated as follows: Cell migration rate (%)=(initial wound area-wound area after 48 h)/initial wound area x100%.

RNA extraction and reverse transcription (RT)-qPCR. RNA extraction was performed as described previously (13). Briefly, total cellular RNA was extracted using TRIzol (cat. no. 15596-018; Invitrogen; Thermo Fisher Scientific, Inc.). RT was performed using the iScript™ cDNA Synthesis kit (cat. no. 1708891, Bio-Rad Laboratories, Inc.) according to the manufacturer's instructions. RT-qPCR assays were performed on a Roche Light Cycler® 96 instrument (LightCycler® 480 II, Roche, Inc.) using a SYBR Green *Pro Taq* HS qPCR kit (cat. no. AG11701, Hunan Aikerui Bioengineering Co., Ltd.). PCR was performed in triplicate. Thermocycling conditions were as follows: Initial denaturation at 95˚C for 30 sec followed by 40 cycles of 95˚C (5 sec) and 60˚C (30 sec). The data were analyzed by the $2^{-\Delta\Delta Cq}$ method (14). U6 was used as an internal reference for the detection of ABHD11-AS1 RNA levels and nuclear ABHD11-AS1. GAPDH was used as an internal reference for cytoplasmic ABHD11-AS1. The primer sequences are listed in Table SII.

Western blotting. Total proteins were lysed using RIPA buffer containing a protease inhibitor cocktail (Beyotime Biotechnology). After quantifying the protein concentration using the BCA) method, protein (30 μg/lane) were separated by SDS-PAGE on a 10% gel and transferred to a PVDF membrane. After blocking with 5% QuickBlock™ Blocking Buffer (cat. no. P0252, Beyotime Institute of Biotechnology) at room temperature for 1 h, the membranes were incubated overnight at 4˚C with primary antibodies (all 1:1,000; see Table SIII). The bound antibodies were detected with horseradish peroxidase-conjugated secondary antibodies (all 1:10,000; Table SIII) for 90 min of incubation at room temperature, and visualized using Pierce™ ECL Western Blotting Substrate (Thermo Fisher Scientific, Inc.). The levels of target proteins were quantified by densitometric scanning using ImageJ software (V1.54d, National Institutes of Health).

RIP. RIP assays were performed using the Magna RIP kit (cat. no. 17-701, MilliporeSigma). Briefly, HCT116 and SW620 cells were lysed with complete RIP lysis buffer (containing inhibitor and RNase), followed by centrifugation at 11,000 x g and 4˚C for 10 min. A total of 10 μl mixture as input was removed, the remaining lysate was mixed with the appropriate antibody (anti-EGFR, 1:20, A11577, ABclonal, 5 ug) and prewashed A/G magnetic beads, and the mixture was incubated overnight at 4˚C. The precipitate was washed with RIP wash buffer, resuspended in 150 μl proteinase K buffer and incubated at 55˚C for 30 min. The products were used for RNA purification by RT-qPCR.

In situ hybridization (ISH). ISH was performed as previously described (15). ABHD11-AS1 transcript levels were assessed in CRC tissues using an ABHD11-AS1-specific probe (5'-DIG-AAGUCUUGUCUGGAAGAGGUGUCUCACUC-3', Sangon Biotech Co., Ltd.). The samples were scored based on staining intensity and the number of positive cells, as described previously (15).

Isolation of cytoplasmic and nuclear fractions. Cytoplasmic and nuclear lysate from HCT116, HT29, SW480 and SW620 cells was separated using a PARIS kit (cat. no. AM1921, Invitrogen; Thermo Fisher Scientific, Inc.) according to the manufacturer's instructions. RNA was extracted from cytoplasmic and nuclear lysates and analyzed by RT-qPCR. The nuclear control transcript was U6; cytoplasmic control transcript was GAPDH.

RNA pull-down assay. RNA pull-down was conducted using Ribo™ RNAmax-T7 Biotin Labeling Transcription kit (cat. no. C11002-1, Guangzhou RiboBio Co., Ltd.). Briefly, PCR primers for the T7 promoter were designed and amplified by PCR (cat. no. AG12210, ApexHF HS DNA Polymerase Premix-CL, Hunan ACCURATE BIOLOGY Co., Ltd.) to obtain DNA templates (sense forward, 5'-TAATACGACTCA CTATAGGGCTAGC-3' and reverse, 5'-CCCCGAGTACCC TTGGC-3'; antisense forward, 5'-TAATACGACTCACTATAG GGCTAGC-3' and reverse, 5'-CCCTAAGTCCCAGCCCTT GA-3'). Cells were lysed with 200 μl lysis buffer for 30 min on ice, followed by centrifugation at 11,000 g for 15 min at 4˚C. Then, 40 μl streptavidin magnetic beads and 10 μl T7 biotin-labeled RNA probe were mixed at 4˚C for 6-8 h to mix the RNA and magnetic beads well. The prepared protein solution lysate was then added to the above RNA magnetic beads and incubated overnight at 4˚C with gentle vortexing to fully bind the RNA to the target protein. PCR reaction was subjected to an initial denaturation at 94˚C for 1 min, followed by 35 cycles of denaturation at 98˚C for 10 sec, and extension at 68˚C for 30 sec. Purified RNA products were obtained by *in vitro* transcription. ABHD11-AS1 intercalating proteins were captured using 40 μl M-280 streptavidin magnetic beads (cat. no. 11205D, Invitrogen; Thermo Fisher Scientific, Inc.) and target proteins were subsequently identified by western blotting (anti-EGFR, 1:1,000, A11577, ABclonal; anti-GAPDH, 1:1,000, 10494-1-AP, Proteintech Group, Inc.).

Bioinformatics analysis. Gene Expression Profiling Interactive Analysis (GEPIA2) (http://gepia2.cancer-pku.cn/#index) database was used to predict the expression of ABHD11-AS1 in colon adenocarcinoma (COAD) and rectal adenocarcinoma (READ) (16). The Cancer Genome Atlas (TCGA; tcga-xena-hub.s3.us-east-1.amazonaws.com/download/survival%2FCOAD_survival.txt) database was used to obtain prognostic information for patients with ABHD11-AS1 and CRC. RPISeq (pridb.gdcb.iastate.edu/RPISeq/) database was used to predict the RNA-binding proteins of ABHD11-AS1 (17).

Statistical analysis. For paired clinical data, matched samples t-test was used. For unpaired data, unpaired Student's t-test was performed. One-way ANOVA followed by Tukey's post hoc test or two-way ANOVA and Sidak's multiple comparison test were used for comparisons between multiple groups. Survival analysis was performed by Kaplan-Meier curves, and the log-rank test was used to determine significance. All the experiments were repeated ≥3 times. All data are expressed

as the mean ± SD and analyzed with GraphPad Prism 8.0 (Dotmatics). P<0.05 was considered to indicate a statistically significant difference.

Results

Downregulation of ABHD11-AS1 transcripts in CRC indicates poor prognosis. To investigate ABHD11-AS1 expression in CRC, GEPIA database was used. ABHD11-AS1 expression was downregulated in COAD tissue (Fig. 1A). ABHD11-AS1 was not significantly downregulated in READ tissues. Compared with those in NCM460 cells, ABHD11-AS1 transcript levels were significantly decreased in CRC cell lines, with those in HCT116 cells decreasing the most and those in SW620 cells decreasing the least (Fig. 1B). Therefore, these cell lines were used for subsequent experiments. Nuclear and cytoplasmic samples were isolated from CRC cell lines; ABHD11-AS1 was localized mainly in the cytoplasm (Fig. S1A-D). ISH of CRC samples revealed that ABHD11-AS1 transcript levels were significantly higher in cancerous (n=66) than in paracancerous tissues (n=39; Fig. 1C-E). By analyzing the clinicopathological characteristics of 66 patients, low ABHD11-AS1 expression was demonstrated to be associated with tumor progression and distant metastasis (Table I). Low ABHD11-AS1 transcript levels were associated with shorter overall survival in patients with CRC in TCGA cohort (Fig. 1F). Together, these findings indicated that downregulated ABHD11-AS1 transcripts are related to poor prognosis in CRC.

ABHD11-AS1 inhibits malignant behaviors of CRC cells in vitro. Given the dysregulated expression of ABHD11-AS1 in CRC, HCT116 and SW620 cells were transfected with plasmids carrying ABHD11-AS1 or ABHD11-AS1 shRNA to test the biological function of ABHD11-AS1. ABHD11-AS1 was successfully overexpressed in HCT116 cells, while transfection with sh-ABHD11-AS1-1, sh-ABHD11-AS1-2 or sh-ABHD11-AS1-3 significantly decreased ABHD11-AS1 expression in SW620 cells by ~99% (Fig. S1E and F). Colony formation and CCK-8 assays revealed that ABHD11-AS1 overexpression inhibited the proliferation of HCT116 cells and ABHD11-AS1 knockdown promoted proliferation of SW620 cells (Fig. 2A-F). Transwell assay revealed that ABHD11-AS1 overexpression significantly inhibited migration and invasion of HCT116 cells, whereas ABHD11-AS1 knockdown significantly promoted migration and invasion capacities of SW620 cells (Fig. 2G-L). Overall, these results indicated ABHD11-AS1 served as a tumor suppressor gene to inhibit proliferation and migration and invasion of CRC cells *in vitro*. Furthermore, wound healing assay revealed that ABHD11-AS1 overexpression inhibited the wound healing process in HCT116 cells. Conversely, ABHD11-AS1 knockdown promoted the wound healing process in SW620 cells (Fig. S2A-D).

To elucidate the function of ABHD11-AS1 in CRC, HCT116 and SW620 cells were transfected with a plasmid encoding ABHD11-AS1 shRNA and expressing ABHD11-AS1. RT-qPCR revealed that compared with control + vector, ABHD11-AS1 expression was effectively downregulated in sh-ABHD11-AS1-2 and ABHD11-AS1-3 groups. ABHD11-AS1 expression was successfully restored in the sh-ABHD11-AS1-2 and sh-ABHD11-AS1-3 + ABHD11-AS1 groups

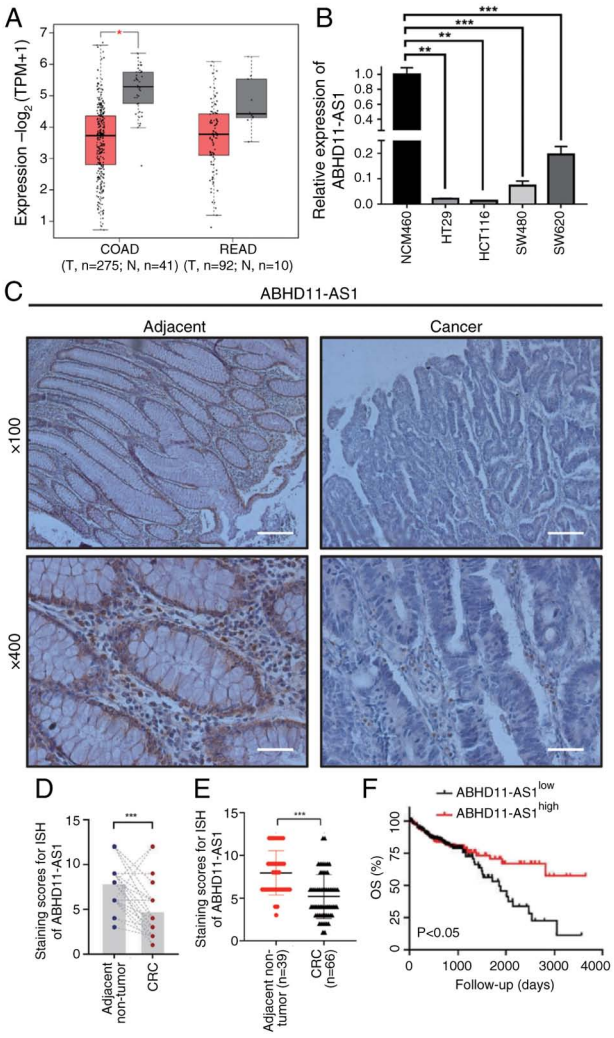

Figure 1. Downregulation of ABHD11-AS1 transcripts is associated with poor prognosis in patients with CRC. (A) ABHD11-AS1 transcript levels in patients with COAD and READ retrieved from the Gene Expression Profiling Interactive Analysis database. (B) Relative levels of ABHD11-AS1 transcripts were determined by reverse transcription-quantitative PCR (n=3). (C) Representative ISH of paraneoplastic and cancerous tissue. ISH staining scores for ABHD11-AS1 in in (D) 39 paired CRC tissues and adjacent paracancerous tissues. (E) ISH staining scores for ABHD11-AS1 in 66 CRC tissues and 39 adjacent paracancerous tissues. (F) Low levels of ABHD11-AS1 transcripts are associated with worse overall survival in patients with CRC in TCGA cohort. Magnification, x100, scale bar=100 μm; magnification, x400, scale bar, 20 μm. *P<0.05, **P<0.01, ***P<0.001. CRC, colorectal cancer; COAD, colon adenocarcinoma; READ, rectal adenocarcinoma; ISH, *in situ* hybridization; T, tumor; N, normal; OS, overall survival; TCGA, The Cancer Genome Atlas; TPM, transcripts per million.

(Fig. S3A and B). Transwell assay revealed that ABHD11-AS1 knockdown promoted migration and invasion of HCT116 and SW620 cells. Notably, this promotion of migration and invasion was inhibited when ABHD11-AS1 expression returned to normal levels (Fig. S3C-H). Wound healing assay revealed that ABHD11-AS1 knockdown promoted migration of HCT116 and SW620 cells. Notably, this was inhibited when ABHD11-AS1 expression returned to normal levels (Fig. S2E-H). CCK-8 assay revealed that ABHD11-AS1 knockdown promoted the proliferation of HCT116 and SW620 cells. Notably, this promotion of proliferation was inhibited when ABHD11-AS1 expression returned to normal levels (Fig. S3I and J).

Table I. Association between clinical parameters with ABHD11-AS1 in patients with colorectal cancer.

Variable	n	High ABHD11-AS1	Low ABHD11-AS1	P-value
Age, years				
<60	40	14	26	0.939
≥60	26	8	18	
Sex				
Male	39	12	27	0.913
Female	27	7	20	
Histology				
Well-differentiated	16	3	13	0.855
Moderately differentiated	35	12	23	
Poorly differentiated	15	5	10	
TNM stage				
I	17	6	11	0.035
II	25	9	16	
III	13	5	8	
IV	11	4	7	
Metastasis				
Yes	43	9	34	0.015
No	23	10	13	

ABHD11-AS1 interacts with EGFR to attenuate EGFR and ERK signaling in CRC cells. To understand the mechanism underlying the role of ABHD11-AS1 in the malignant biological behavior of CRC, RPISeq database was used to predict the RNA-binding proteins of ABHD11-AS1. ABHD11-AS1 bound to EGFR (random forest classifier, 0.8; support vector machine classifier, 0.65; Fig. 3A). RNA pull-down and RIP assay confirmed the interactions between ABHD11-AS1 and EGFR (Fig. 3B-D). Furthermore, immunofluorescence revealed colocalization of ABHD11-AS1 and EGFR in the cytoplasm (Fig. 3E). These results indicated that ABHD11-AS1 interacted with EGFR.

To investigate the molecular mechanism, ABHD11-AS1 was overexpressed or knocked down in HCT116 and SW620 cells prior to detecting proteins associated with the EGFR/ERK signaling pathway as this pathway is key for tumor progression (18). Western blot analysis revealed that transfection with ABHD11-AS1 plasmid decreased phosphorylation of EGFR and ERK1/2 (Figs. 3F and S4A and B). Conversely, sh-ABHD11-AS1 plasmid increased the phosphorylation of EGFR and ERK1/2 (Figs. 3F and S4C and D). These results indicated that interaction between ABHD11-AS1 and EGFR resulted in attenuation of ERFR/ERK signaling.

EGFR activation abrogates ABHD11-AS1-mediated attenuation of proliferative and migratory behaviors in CRC cells. To confirm that ABHD11-AS1 inhibited proliferative and migratory behaviors of CRC cells via EGFR, CRC cells with stably altered ABHD11-AS1 expression were treated with the EGFR agonist NSC228155 or inhibitor chrysophanol. Compared with control, NSC228155 increased EGFR and ERK1/2 phosphorylation but had no effect on total EGFR or ERK1/2 protein expression (Figs. 4A and S4E and F). NSC228155 almost completely restored ABHD11-AS1-attenuated EGFR and ERK1/2 phosphorylation (Figs. 4A and S4E and F). Similarly, chrysophanol attenuated EGFR and ERK1/2 phosphorylation but not total protein expression (Figs. 4B and S4G and H). Chrysophanol almost completely abrogated sh-ABHD11-AS1-induced increases in EGFR and ERK1/2 phosphorylation (Figs. 4B and S4G and H).

It was hypothesized that ABHD11-AS1 inhibits CRC cell proliferation and invasion by impairing EGFR phosphorylation and EGFR signaling. Compared with control, NSC228155 promoted the proliferation, migration and invasion of HCT116 cells *in vitro*. NSC228155 almost completely reversed ABHD11-AS1-mediated inhibition of proliferation, migration and invasion (Figs. 4C, E, G, I and J and S5A). Chrysophanol inhibited proliferation, migration and invasion of SW620 cells *in vitro* (Figs. 4D, F, H, K and L and S4B). Furthermore, chrysophanol inhibited proliferation, migration and invasion of SW620 cells induced by ABHD11-AS1 knockdown. These results indicated that the ABHD11-AS1/EGFR signaling axis plays a role in regulating malignant behavior of CRC cells.

Resveratrol enhances ABHD11-AS1 transcript levels to suppress malignant behavior of CRC cells by downregulating SPT6. The aforementioned results indicated ABHD11-AS1 had a tumor-suppressive effect on CRC. To explore therapeutic approaches for CRC that target ABHD11-AS1, resveratrol was investigated as a potential regulator of ABHD11-AS1 (19,20). RSV can exert antitumor effects by altering lncRNA transcript levels (21). To investigate the potential association between RSV and ABHD11-AS1 transcript levels, HCT116 and SW620 cells were treated with RSV.

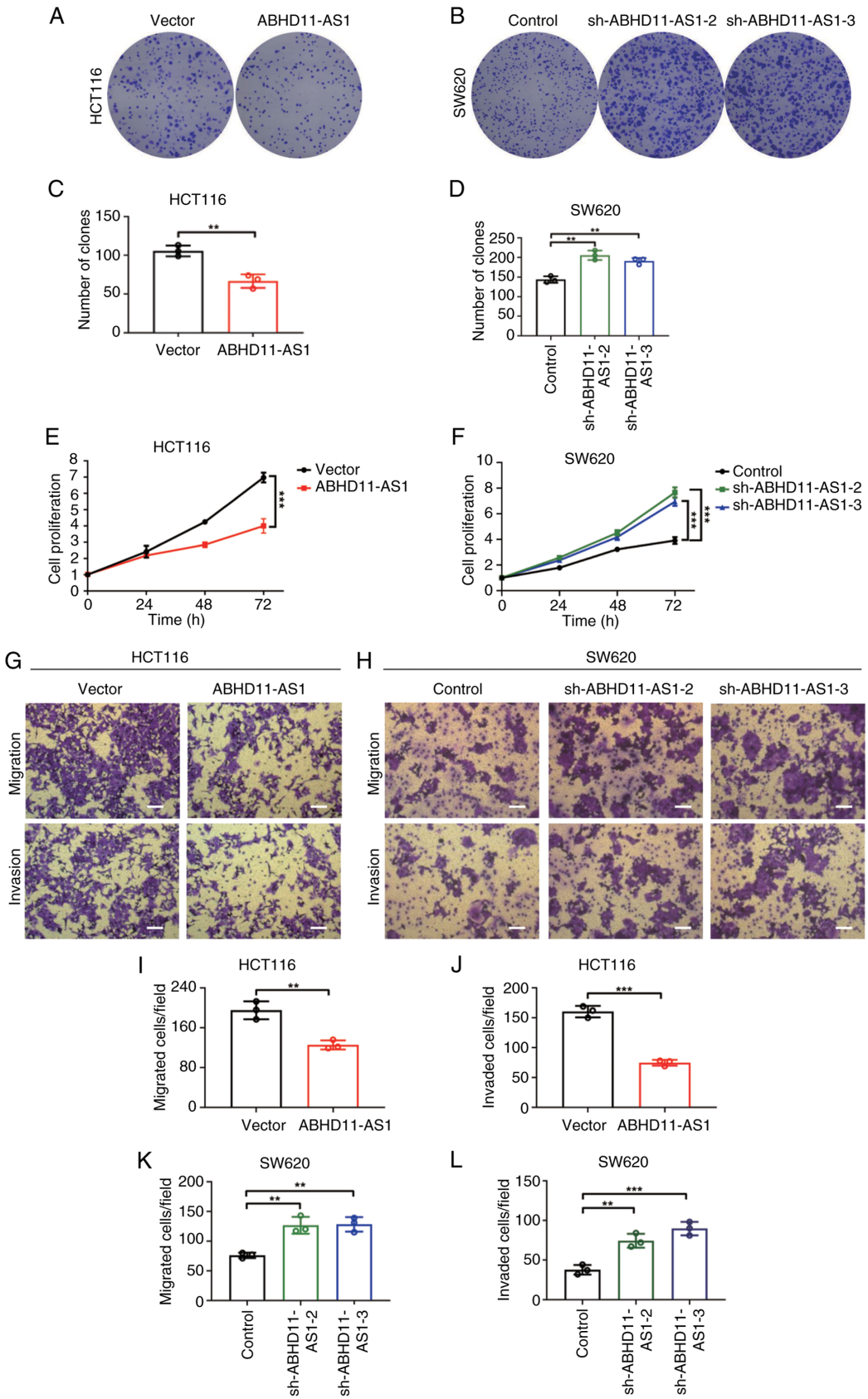

Figure 2. ABHD11-AS1 attenuates proliferative and migratory behaviors of CRC cells *in vitro*. (A) Colony formation assays in ABHD11-AS1 overexpressing HCT116 cells. (B) Colony formation assays in ABHD11-AS1 knockdown SW620 cells. (C) Statistical graphs of colony formation assays in ABHD11-AS1 overexpressing HCT116 cells. (D) Statistical graphs of colony formation assays in ABHD11-AS1 knockdown SW620 cells. (E) CCK-8 assays in ABHD11-AS1 overexpressing HCT116 cells. (F) CCK-8 assays in ABHD11-AS1 knockdown SW620 cells. (G) Transwell migration and invasion assays in ABHD11-AS1 overexpressing HCT116 cells. (H) Transwell migration and invasion assays ABHD11-AS1 knockdown SW620 cells. (I) Statistical graphs of Transwell migration assays in ABHD11-AS1 overexpressing HCT116 cells. (J) Statistical graphs of Transwell invasion assays in ABHD11-AS1 overexpressing HCT116 cells. (K) Migration assays in ABHD11-AS1 knockdown SW620 cells. (L) Invasion ability of ABHD11-AS1 knockdown SW620 cells. Magnification, x200. Scale bar: 50 μm. **P<0.01, ***P<0.001. CRC, colorectal cancer; sh, short hairpin.

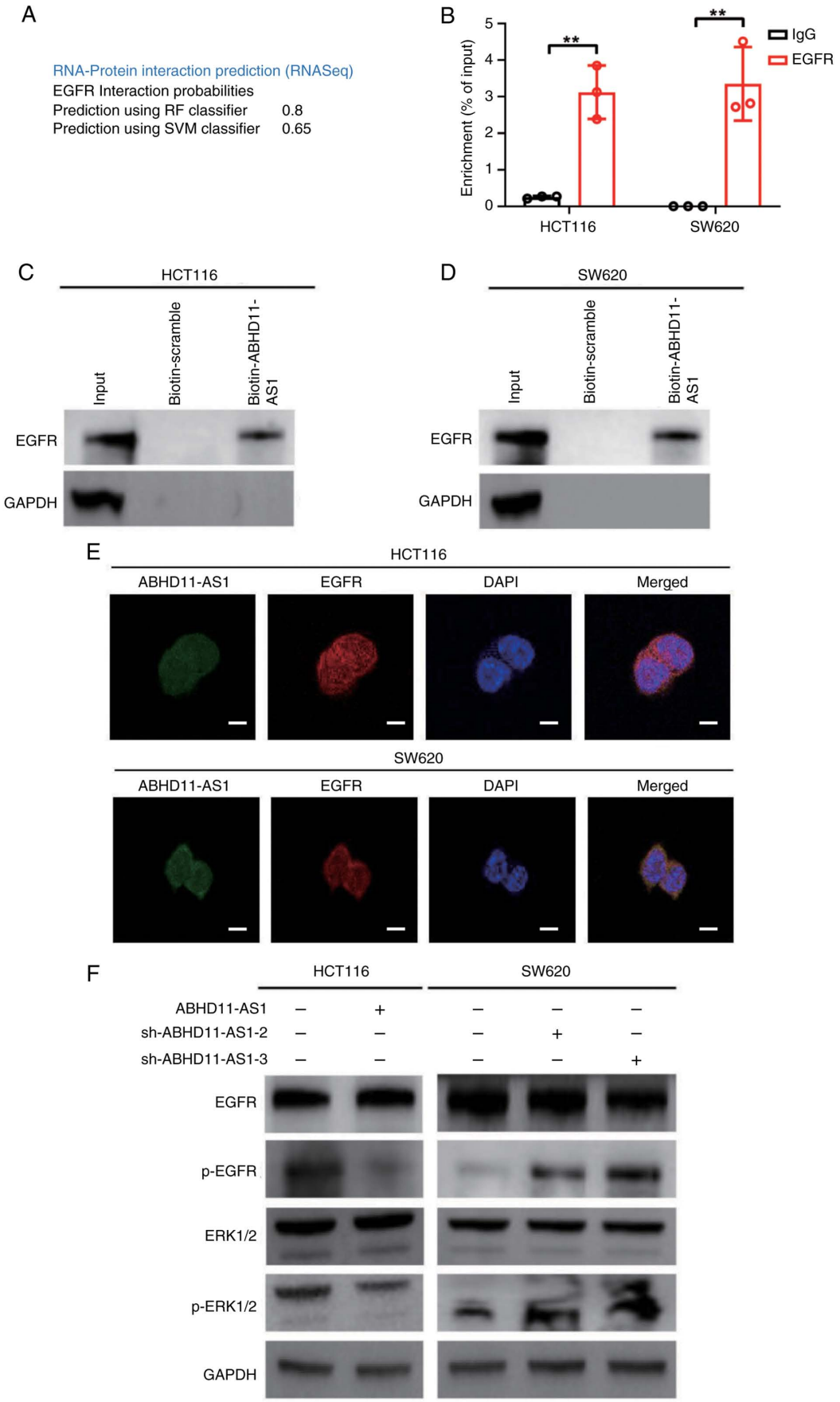

Figure 3. ABHD11-AS1 interacts with EGFR and decreases EGFR phosphorylation. (A) RPISeq database was used to predict ABHD11-AS1-interacting proteins. (B) RIP assay revealed an interaction between EGFR and ABHD11-AS1 in HCT116 and SW620 cells. (C) RNA pull-down revealed an interaction between ABHD11-AS1 and EGFR in HCT116 cells. (D) RNA pull-down revealed an interaction between ABHD11-AS1 and EGFR in SW620 cells. (E) Colocalization of ABHD11-AS1 with EGFR. Scale bar, 5 μm. (F) Western blot analysis was conducted to assess the impact of altered ABHD11-AS1 expression on EGFR and ERK1/2 expression and phosphorylation. p-, phosphorylated; RF, random forest; SVM, support vector machine; sh, short hairpin. **P<0.01.

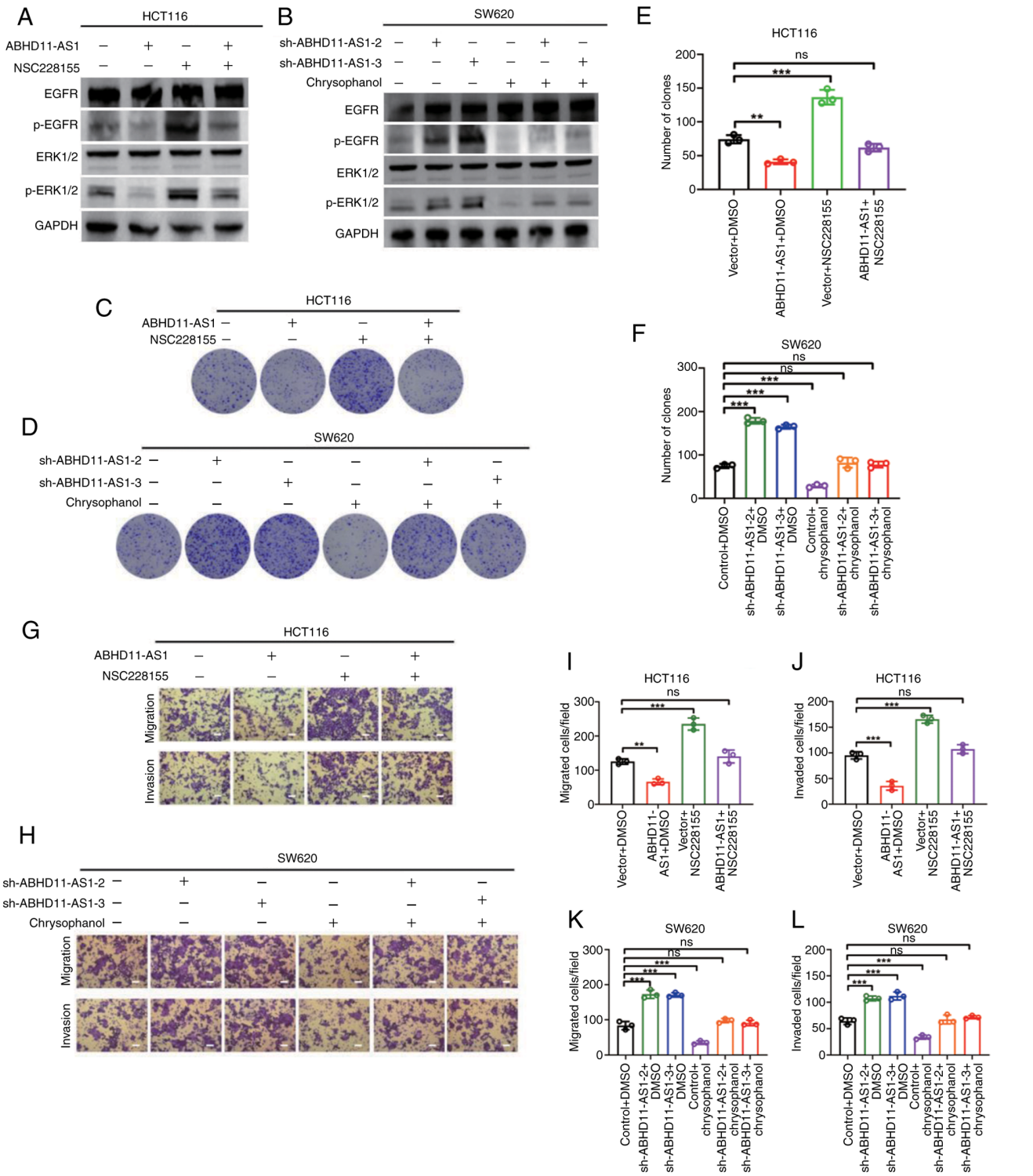

Figure 4. Induction of EGFR overexpression abrogates ABHD11-AS1-mediated attenuation of proliferative and migratory behaviors in CRC cells. ABHD11-AS1 was overexpressed or knocked down in HCT116 and SW620 cells, respectively, and NSC228155 and chrysophanol were administered. (A) Western blot analysis of EGFR, ERK1/2, and EGFR and ERK1/2 phosphorylation in (A) HCT116 cells. (B) Western blot analysis of EGFR, ERK1/2, and EGFR and (B) SW620 cells. (C) Effects of NSC228155 on colony formation capacities in HCT116 cells. (D) Effects of chrysophanol on colony formation capacities in SW620 cells. (E) Statistical graphs of colony formation assays in HCT116 cells. (F) Statistical graphs of colony formation assays in SW620 cells. (G) Effects of NSC228155 on migration and invasion capacities of HCT116 cells. (H) Effects of chrysophanol on migration and invasion capacities of SW620 cells. (I) Statistical graphs of Transwell migration assays in HCT116 cells. (J) Statistical graphs of Transwell invasion assays in HCT116 cells. (K) Migration assays in SW620 cells. (L) Statistical graphs of Transwell invasion assays in SW620 cells. Scale bar, 50 μm. **P<0.01, ***P<0.001. CRC, colorectal cancer; p-, phosphorylated; ns, not significant; sh, short hairpin.

As RSV has varying degrees of cytotoxicity (22), half-maximal inhibitory concentration (IC50) values of RSV in HCT116 and SW480 cells were calculated. IC50 values of RSV were 57.16 in HCT116 and 65.12 μM in SW480 cells (Fig. 5A and B). CRC cell viability was inhibited by RSV *in vitro*, with a mean IC50 value of 60 μM.

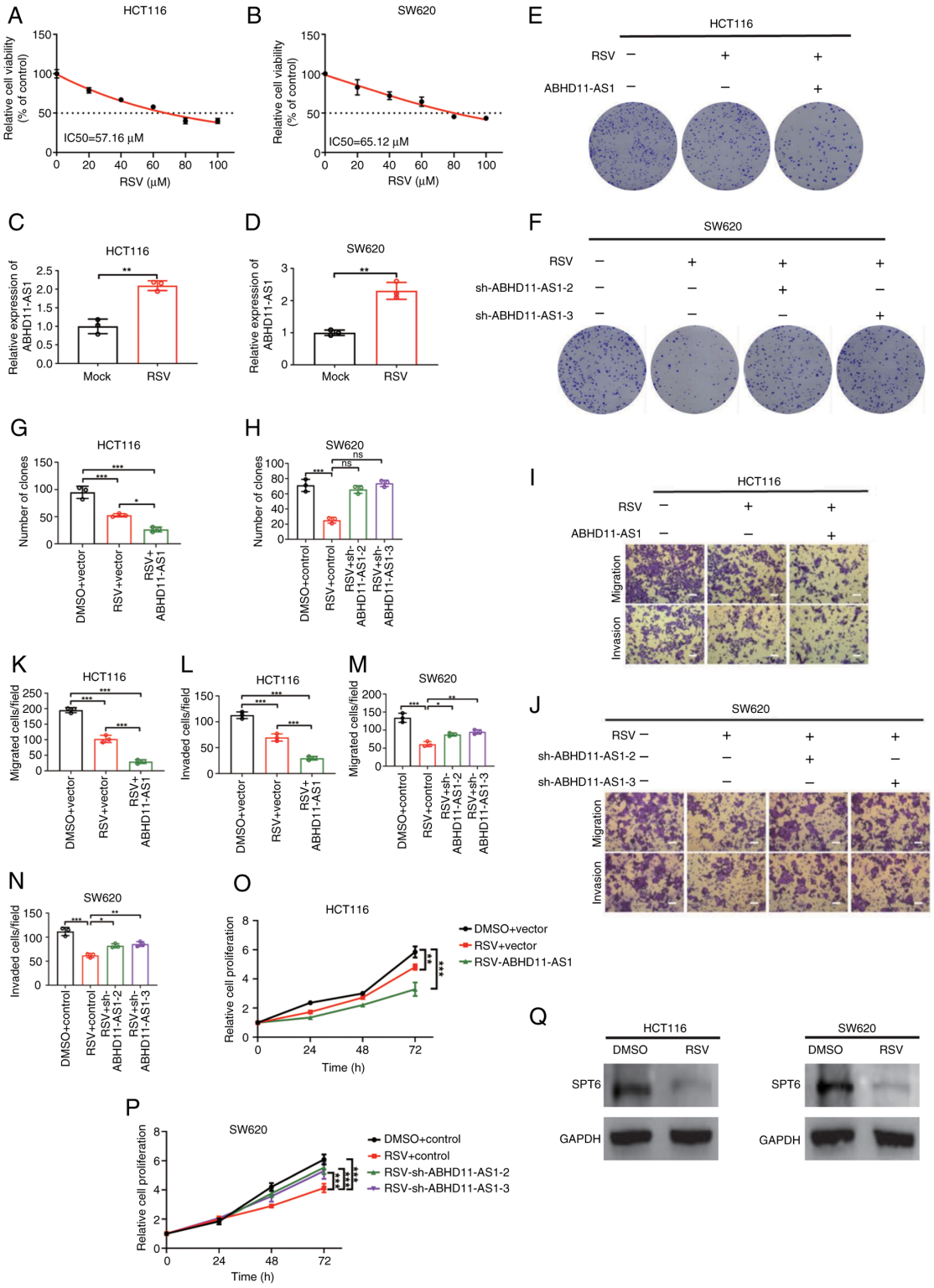

Figure 5. RSV decreases SPT6 protein and promotes ABHD11-AS1 transcript levels to inhibit colorectal cancer progression. (A) HCT116 cells were treated with RSV and assayed for viability to calculate the IC50 values. (B) SW620 cells were treated with RSV and assayed for viability to calculate the IC50 values. (C) RT-qPCR was used to assess the impact of RSV on ABHD11-AS1 transcript levels in HCT116 cells. (D) RT-qPCR was used to assess the impact of RSV on ABHD11-AS1 transcript levels in SW620 cells. (E) ABHD11-AS1 overexpression plasmid was transfected into RSV-treated HCT116 cells and colony formation was detected. (F) ABHD11-AS1 interference plasmid was transfected into RSV-treated SW620 cells and colony formation capacities were detected. (G) Statistical graphs of colony formation assays in HCT116 cells. (H) Statistical graphs of colony formation assays in SW620 cells. (I) ABHD11-AS1 overexpression plasmid was transfected into RSV-treated HCT116 cells and migration and invasion capacities were detected. (J) ABHD11-AS1 interference plasmid was transfected into RSV-treated SW620 cells and migration and invasion capacities were detected. (K) Statistical graphs of Transwell migration assays in HCT116 cells. (L) Statistical graphs of Transwell invasion assays in HCT116 cells. (M) Statistical graphs of Transwell migration assays in SW620 cells. (N) Statistical graphs of Transwell invasion assays in HCT116 cells. (O) ABHD11-AS1 overexpression plasmid was transfected into RSV-treated HCT116 cells and proliferation capacities were detected. (P) ABHD11-AS1 interference plasmid was transfected into RSV-treated SW620 cells and proliferation capacities were detected. Scale bar, 50 μm. (Q) Western blot analysis was conducted to determine the effect of RSV on SPT6 protein levels. *P<0.05, **P<0.01, ***P<0.001. RSV, resveratrol; SPT6, SPT6 homolog, histone chaperone and transcription elongation factor; IC50, half maximal inhibitory concentration; sh, short hairpin; ns, not significant.

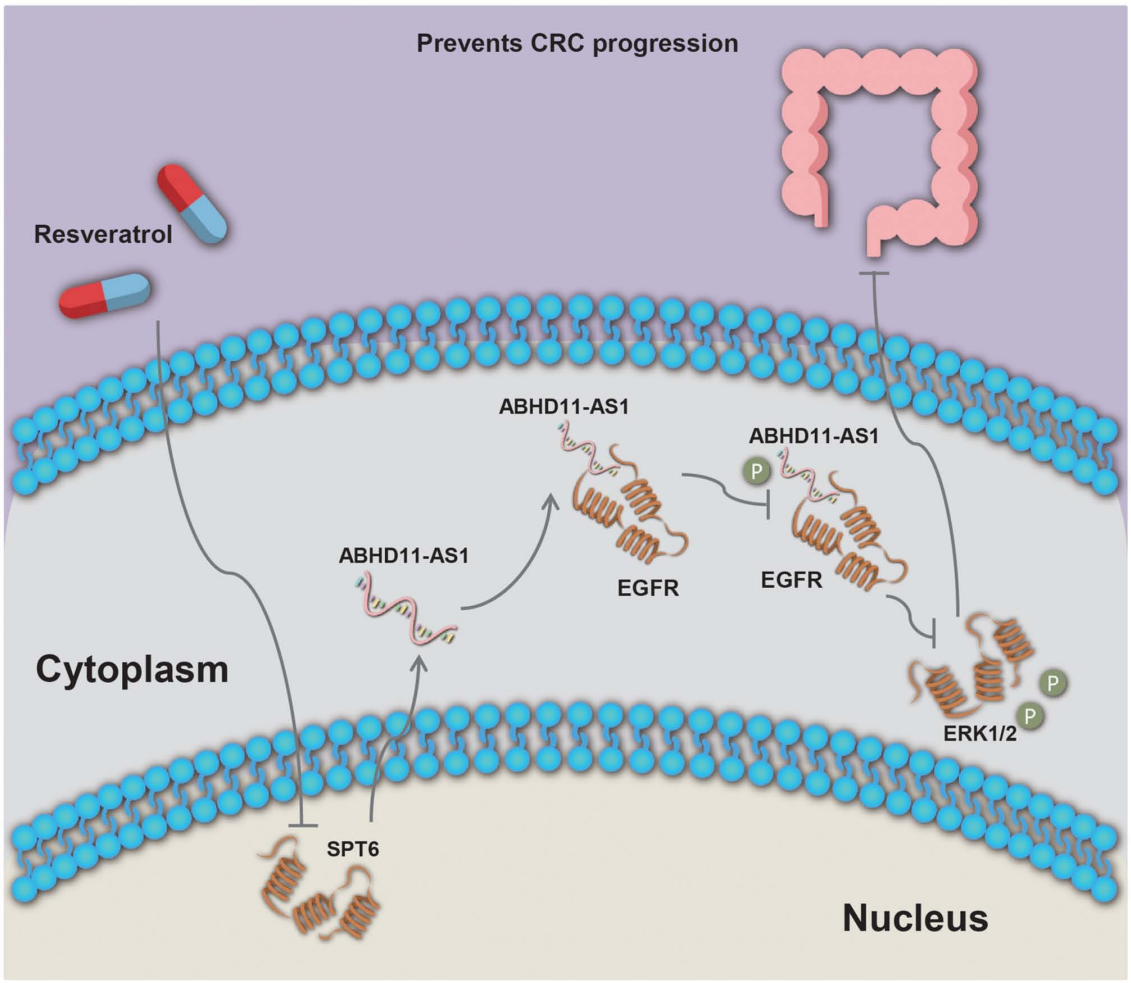

Figure 6. Molecular mechanism by which ABHD11-AS1 inhibits CRC progression. ABHD11-AS1 binds EGFR and inhibits the proliferation and metastasis of CRC cells by suppressing the EGFR/ERK signaling pathway. Resveratrol decreases SPT6 protein expression and increases transcript levels of ABHD11-AS1, suggesting its potential application in CRC treatment. CRC, colorectal cancer; SPT6, SPT6 homolog, histone chaperone and transcription elongation factor.

RSV significantly increased transcript levels of ABHD11-AS1 (Fig. 5C and D). Furthermore, RSV did not affect the subcellular localization of ABHD11-AS1 (Fig. S1G and H). To assess whether altered ABHD11-AS1 transcript levels influenced effects of RSV, RSV-treated HCT116 and SW480 cells were transfected with plasmids carrying ABHD11-AS1 or ABHD11-AS1 shRNA. Compared with control, RSV significantly inhibited proliferation, colony formation, wound healing, migration and invasion of HCT116 and SW620 cells (Fig. 5E, G-I, K, L and O). ABHD11-AS1 overexpression further enhanced the inhibitory effects of RSV on HCT116 cell proliferation, colony formation, wound healing, migration and invasion. By contrast, ABHD11-AS1 knockdown abolished the inhibitory effects of RSV on SW480 cell proliferation, colony formation, wound healing, migration and invasion (Fig. 5F, H, J, M, N and P). These results indicated that RSV inhibited proliferation, migration and invasion of HCT116 and SW480 cells by increasing ABHD11-AS1 transcript levels.

These data suggested that RSV increased ABHD11-AS1 transcript levels. A decrease in SPT6 expression results in conversion of the H3K36me3 histone mark from protein-coding to lncRNA-coding, which is associated with increased lncRNA transcription (23,24). Western blotting results suggested that RSV could reduce SPT6 protein expression (Fig. 5Q). These results indicated that RSV may exert antitumor effects by inducing SPT6 protein deletion.

Discussion

CRC is one of the three most common types of cancer in the world (2). A total of ~60% of patients with CRC have insidious presentation and the 5-year survival rate is 30-40% (25); thus, there is need to develop novel therapeutic targets to promote early diagnosis and precision treatment of CRC (Fig. 6).

lncRNAs serve roles in regulating expression of genes that are involved in tumor progression (26). Recent studies have shown that CCAT1, H19 and SNHG6, which are notably overexpressed in peripheral blood or cancer tissue of patients with CRC, are potential biomarkers for diagnosis and prognostic assessment of CRC (27-29). In addition, autophagy-, pyroptosis- and EMT-associated lncRNAs may serve as biomarkers for diagnosis and prognosis of CRC (30-32).

Dysregulated expression of lncRNAs contributes to tumor progression. lncRNAs serve opposite roles in different types of cancer. For example, H19 is highly expressed in skin squamous cell carcinoma tissue and cell lines and promotes cancer

cell migration and invasion by inhibiting p53 expression (33). A study on osteosarcoma revealed that lncRNA H19 inhibits SNORA7A expression to suppress osteosarcoma progression (9). lncRNA TINCR has been widely reported to be an oncogene that promotes the progression of numerous types of tumors (including cervical and colon cancer and hepatocellular carcinomas) (34-36). However, TINCR can act as a tumor suppressor gene and inhibit the proliferation and metastasis of laryngeal squamous cell carcinoma cells by regulating the miR-210/anti-proliferation factor 2 axis (37). PVT1 was the first reported tumor-associated lncRNA with pro-oncogenic functions in various types of tumor (38,39). Promoter of PVT1 functions as a tumor suppressor DNA element because MYC is located on the same TAD structure as PVT1 (40). SNHG1 is associated with growth, metastasis, ferroptosis and chemoresistance in various types of tumor (41,42). There are various perspectives on the role of SNHG1 in gastric cancer. One study reported that SNHG1 serves as a sponge for miR-195-5p, targeting Yes-associated protein 1 to promote the proliferation of gastric cancer cells (43). Another study demonstrated that SNHG1 inhibits invasion of gastric cancer cells by regulating the suppressor of cytokine signaling 2/JAK2/STAT pathway (44). Here, ABHD11-AS1 expression was downregulated in TCGA COAD and READ datasets compared with normal dataset. The present experiments confirmed that ABHD11-AS1 has an antitumor function. Although other studies (45,46) have demonstrated that ABHD11-AS1 expression is elevated in TCGA COAD and READ data relative to TCGA and Genotype-Tissue Expression (GTEx) normal data, this may be attributed to differences in the cited sources, as GTEx encompasses 54 distinct tissue organ sites (such as brain and whole blood).

ABHD11-AS1 interacts with and upregulates cyclin D1 in endometrial cancer (47). The ABHD11-AS1/miR-1231/cyclin E1 axis may regulate the proliferation of pancreatic cancer cells (48). Notably, knockdown of ABHD11-AS1 and EGFR inhibits proliferation of cervical cancer SiHa and Hela cells by downregulating cyclin D1 (49). To the best of our knowledge, there is a lack of evidence indicating a direct impact of ABHD11-AS1 on expression of cyclin superfamily proteins in CRC cells and associations between ABHD11-AS1 and cyclin-dependent kinase, cyclin-dependent kinase inhibitor (CKI) and cyclin-dependent kinase activating kinase (CAK) superfamily proteins; however, it is hypothesized that ABHD11-AS1 may influence the cell cycle in CRC (50).

RSV is a polyphenolic antioxidant with a wide range of functions, including anti-inflammatory and antioxidant effects (51). It also inhibits tumor growth and prevents tumorigenesis. RSV inhibits the proliferation and invasion of colon cancer cells and promotes apoptosis by modulating EMT, activating the BMP/Smad signaling and reactive oxygen species-mediated mitochondrial apoptosis pathway (20,52). Notably, RSV may exert antitumor effects by altering lncRNA expression. For example, RSV modulates the expression of the lncRNA ZFAF1, thereby enhancing the efficacy of paclitaxel in non-small cell lung cancer (53). The antitumor effect of RSV in CRC was first reported to involve the inhibition of cancer cell invasion and metastasis via downregulation of lncRNA MALAT1 (54). These findings suggest that RSV may have potential as a therapeutic agent for CRC. Combination of RSV and BIBR1532 (a telomerase inhibitor) exerts an antiproliferative effect by downregulating expression of lncRNAs, including CCAT1, CRNDE, HOTAIR, PCAT1, PVT1 and SNHG16 (55). Here, RSV enhanced ABHD11-AS1 transcript levels to suppress the malignant behavior of CRC cells, which may be mediated by SPT6 deletion.

SPT6 is a conserved histone chaperone and transcription elongation factor that serves a key role in the transcription elongation process (56). Recent studies have also demonstrated its impact on lncRNA transcription. The phosphorylation of RNA polymerase II, coupled with loss of SPT6 expression, may promote transcription of lncRNAs (23,57,58). Decreased SPT6 expression leads to the conversion of the H3K36me3 histone mark from protein- to lncRNA-coding, potentially increasing lncRNA transcription (23). In RSV-treated HCT116 and SW620 cells, SPT6 was downregulated. Silencing SPT6 has been shown to inhibit the growth and metastasis of human-derived colon cancer cell xenograft tumors (59). These results suggest that RSV may target ABHD11-AS1 via SPT6 to exert an antitumor effect.

To investigate potential downstream molecules of ABHD11-AS1, the present study conducted bioinformatics analysis and identified EGFR as one of its interacting proteins. Previous studies have shown that ABHD11-AS1 regulates expression and phosphorylation of EGFR (49,60,61). Furthermore, RNA pull-down and RIP assays revealed formation of lncRNA-protein complexes between ABHD11-AS1 and EGFR. Induction of EGFR overexpression impaired the tumor-suppressive effect of ABHD11-AS1 in CRC cells. EGFR is a key target for the clinical treatment of CRC, as it is generally highly expressed in patients with CRC (62). The present results indicated that downregulation of ABHD11-AS1 expression may be a causative factor for EGFR phosphorylation upregulation in CRC.

In summary, ABHD11-AS1 inhibited proliferation and invasion of CRC cells by binding EGFR proteins and suppressing EGFR phosphorylation. In addition, RSV increased ABHD11-AS1 transcript levels, which inhibited proliferation and invasion of CRC cells. The present findings may provide novel biomarkers for CRC prognosis and new targets for CRC treatment.

Acknowledgements

Not applicable.

Funding

The present study was supported by National Natural Science Foundation of China (grant nos. 82302987, 82303534, 82203233, 82202966 and 82173142), Natural Science Foundation of Hunan Province (grant nos. 2023JJ60469, 2023JJ40413, 2023JJ30372, 2023JJ30375, 2022JJ80078 and 2020JJ5336), Key Research and Development Program of Hunan Province (grant no. 2022SK2051), Science and Technology Innovation Program of Hunan Province (grant nos. 2023RC3199, 2023SK4034 and 2023RC1073), Research Project of Health Commission of Hunan Province (grant nos. 202203034978, 202202055318, 202109031837, 202109032010 and 20201020), Changsha Science and Technology Board (grant no. kh2201054), Ascend Foundation

of the National Cancer Center (grant no. NCC201909B06) and Hunan Cancer Hospital Climb Plan (grant nos. ZX2020001-3, YF2020002, 2023NSFC-A001, 2023NSFC-A002 and 2023NSFC-A004).

Availability of data and materials

The data generated in the present study may be requested from the corresponding author.

Authors' contributions

ST and SL confirm the authenticity of all the raw data. ST and SL drafted the manuscript and constructed the figures. LX, XJ, ZR, QP, MP, WY, XX, LO, MS, JW, HL and YT performed the literature review. QL, JL and YZ designed the study and revised the manuscript. All authors have read and approved the final manuscript. ST conceived the study, conducted formal analysis and performed experiments. SL conceptualized the study.

Ethics approval and consent to participate

The present study was approved by the Ethics Committee of Hunan Cancer Hospital (approval no. KYJJ-2022-240). All participants provided written informed consent.

Patient consent for publication

Not applicable.

Competing interests

The authors declare that they have no competing interests.

References

1. Hang D, Sun D, Du L, Huang J, Li J, Zhu C, Wang L, He J, Zhu X, Zhu M, *et al*: Development and evaluation of a risk prediction tool for risk-adapted screening of colorectal cancer in China. Cancer Lett 597: 217057, 2024.
2. Siegel RL, Wagle NS, Cercek A, Smith RA and Jemal A: Colorectal cancer statistics, 2023. CA Cancer J Clin 73: 233-254, 2023.
3. Liu S, Jiao B, Zhao H, Liang X, Jin F, Liu X and Hu JF: LncRNAs-circRNAs as rising epigenetic binary superstars in regulating lipid metabolic reprogramming of cancers. Adv Sci (Weinh) 11: e2303570, 2024.
4. Yin H, Gu S, Li G, Yu H, Zhang X and Zuo Y: Long noncoding RNA PVT1 predicts poor prognosis and promotes the progression of colorectal cancer through the miR-24-3p/NRP1 axis in zebrafish xenografts. Neoplasma 70: 500-513, 2023.
5. Ren G, Li H, Hong D, Hu F, Jin R, Wu S, Sun W, Jin H, Zhao L, Zhang X, *et al*: LINC00955 suppresses colorectal cancer growth by acting as a molecular scaffold of TRIM25 and Sp1 to Inhibit DNMT3B-mediated methylation of the PHIP promoter. BMC Cancer 23: 898, 2023.
6. Chen ZH, Lin YL, Chen SQ and Yang XY: Identification of necroptosis-related lncRNAs for prognosis prediction and screening of potential drugs in patients with colorectal cancer. World J Gastrointest Oncol 15: 1951-1973, 2023.
7. Mao R, Xu C, Zhang Q, Wang Z, Liu Y, Peng Y and Li M: Predictive significance of glycolysis-associated lncRNA profiles in colorectal cancer progression. BMC Med Genomics 17: 112, 2024.
8. Zhang W, Zhou K, Zhang X, Wu C, Deng D and Yao Z: [Corrigendum] Roles of the H19/microRNA-675 axis in the proliferation and epithelial-mesenchymal transition of human cutaneous squamous cell carcinoma cells. Oncol Rep 50: 149, 2023.
9. Xu A, Huang MF, Zhu D, Gingold JA, Bazer DA, Chang B, Wang D, Lai CC, Lemischka IR, Zhao R and Lee DF: LncRNA H19 suppresses osteosarcomagenesis by regulating snoRNAs and DNA repair protein complexes. Front Genet 11: 611823, 2021.
10. Qiao X, Lv SX, Qiao Y, Li QP, Ye B, Wang CC and Miao L: Long noncoding RNA ABHD11-AS1 predicts the prognosis of pancreatic cancer patients and serves as a promoter by activating the PI3K-AKT pathway. Eur Rev Med Pharmacol Sci 22: 8630-8639, 2018.
11. Zhou X, Zhong F, Yan Y, Wu S, Wang H, Liu J, Li F, Cui D and Xu M: Pancreatic cancer cell-derived exosomes promote lymphangiogenesis by downregulating ABHD11-AS1 expression. Cancers (Basel) 14: 4612, 2022.
12. Xia L, Lin J, Peng M, Jiang X, Peng Q, Cui S, Zhang W, Li S, Wang J, Oyang L, *et al*: Diallyl disulfide induces DNA damage and growth inhibition in colorectal cancer cells by promoting POU2F1 ubiquitination. Int J Biol Sci 20: 1125-1141, 2024.
13. Lin J, Xia L, Oyang L, Liang J, Tan S, Wu N, Yi P, Pan Q, Rao S, Han Y, *et al*: The POU2F1-ALDOA axis promotes the proliferation and chemoresistance of colon cancer cells by enhancing glycolysis and the pentose phosphate pathway activity. Oncogene 41: 1024-1039, 2022.
14. Livak KJ and Schmittgen TD: Analysis of relative gene expression data using real-time quantitative PCR and the 2(-Delta Delta C(T)) method. Methods 25: 402-408, 2001.
15. Yang W, Tan S, Yang L, Chen X, Yang R, Oyang L, Lin J, Xia L, Wu N, Han Y, *et al*: Exosomal miR-205-5p enhances angiogenesis and nasopharyngeal carcinoma metastasis by targeting desmocollin-2. Mol Ther Oncolytics 24: 612-623, 2022.
16. Tang Z, Kang B, Li C, Chen T and Zhang Z: GEPIA2: An enhanced web server for large-scale expression profiling and interactive analysis. Nucleic Acids Res 47 (W1): W556-W560, 2019.
17. Muppirala UK, Honavar VG and Dobbs D: Predicting RNA-protein interactions using only sequence information. BMC Bioinformatics 12: 489, 2011.
18. Wang K, Chu Y, Zhang H, Qu X, Wang B and Han Y: FOXD3 suppresses the proliferation of CRC bone metastatic cells via the Ras/Raf/MEK/ERK signaling pathway. Comb Chem High Throughput Screen 27: 436-445, 2024.
19. Liu Z, Zhang Z, Song G, Wang X, Xing H and Wang C: Resveratrol alleviates skeletal muscle insulin resistance by downregulating long noncoding RNA. Int J Endocrinol 2022: 2539519, 2022.
20. Vernousfaderani EK, Akhtari N, Rezaei S, Rezaee Y, Shiranirad S, Mashhadi M, Hashemi A, Khankandi HP and Behzad S: Resveratrol and colorectal cancer: A molecular approach to clinical researches. Curr Top Med Chem 21: 2634-2646, 2021.
21. Yang Q, Xu E, Dai J, Liu B, Han Z, Wu J, Zhang S, Peng B, Zhang Y and Jiang Y: A novel long noncoding RNA AK001796 acts as an oncogene and is involved in cell growth inhibition by resveratrol in lung cancer. Toxicol Appl Pharmacol 285: 79-88, 2015.
22. Djaldetti M: Immunomodulatory and chemopreventive effects of resveratrol on the digestive system cancers. Oncol Res 32: 1389-1399, 2024.
23. Nojima T, Tellier M, Foxwell J, Ribeiro de Almeida C, Tan-Wong SM, Dhir S, Dujardin G, Dhir A, Murphy S and Proudfoot NJ: Deregulated expression of mammalian lncRNA through loss of SPT6 induces R-loop formation, replication stress, and cellular senescence. Mol Cell 72: 970-984.e7, 2018.
24. Begum NA, Stanlie A, Nakata M, Akiyama H and Honjo T: The histone chaperone Spt6 is required for activation-induced cytidine deaminase target determination through H3K4me3 regulation. J Biol Chem 287: 32415-32429, 2012.
25. Zeng H, Chen W, Zheng R, Zhang S, Ji JS, Zou X, Xia C, Sun K, Yang Z, Li H, *et al*: Changing cancer survival in China during 2003-15: A pooled analysis of 17 population-based cancer registries. Lancet Glob Health 6: e555-e567, 2018.
26. Zhu P, Liu B and Fan Z: Noncoding RNAs in tumorigenesis and tumor therapy. Fundam Res 3: 692-706, 2023.
27. Li B, Zheng L, Ye J, Zhang C, Zhou J, Huang Q, Guo Y, Wang L, Yu P, Liu S, *et al*: CREB1 contributes colorectal cancer cell plasticity by regulating lncRNA CCAT1 and NF-κB pathways. Sci China Life Sci 65: 1481-1497, 2022.
28. Chowdhury PR, Salvamani S, Gunasekaran B, Peng HB and Ulaganathan V: H19: An oncogenic long non-coding RNA in colorectal cancer. Yale J Biol Med 96: 495-509, 2023.

29. Jurkiewicz M, Szczepaniak A and Zielinska M: Long non-coding RNAs-SNHG6 emerge as potential marker in colorectal cancer. Biochim Biophys Acta Rev Cancer 1879: 189056, 2024.
30. Zhao D, Sun X, Long S and Yao S: An autophagy-related long non-coding RNA signature for patients with colorectal cancer. Physiol Int: Jul 5, 2021 (Epub ahead of print).
31. Chen S, Zhu J and Zhi X: A novel pyroptosis-associated long noncoding RNA signature to predict the prognosis of patients with colorectal cancer. Int J Gen Med 14: 6111-6123, 2021.
32. Zhang S, Fan W and He D: Constructing a personalized prognostic risk model for colorectal cancer using machine learning and multi-omics approach based on epithelial-mesenchymal transition-related genes. J Gene Med 26: e3660, 2024.
33. Zhang W, Zhou K, Zhang X, Wu C, Deng D and Yao Z: Roles of the H19/microRNA-675 axis in the proliferation and epithelial-mesenchymal transition of human cutaneous squamous cell carcinoma cells. Oncol Rep 45: 39, 2021.
34. Ren Z, Liu J, Li J and Yao L: Decreased lncRNA, TINCR, promotes growth of colorectal carcinoma through upregulating microRNA-31. Aging (Albany NY) 12: 14219-14231, 2020.
35. Liu X, Wang CX, Feng Q and Zhang T: lncRNA TINCR promotes the development of cervical cancer via the miRNA-7/mTOR axis *in vitro*. Exp Ther Med 26: 487, 2023.
36. Shi J, Guo C, Li Y and Ma J: The long noncoding RNA TINCR promotes self-renewal of human liver cancer stem cells through autophagy activation. Cell Death Dis 13: 961, 2022.
37. He G, Pang R, Han J, Jia J, Ding Z, Bi W, Yu J, Chen L, Zhang J and Sun Y: TINCR inhibits the proliferation and invasion of laryngeal squamous cell carcinoma by regulating miR-210/BTG2. BMC Cancer 21: 753, 2021.
38. Li G, Feng J, Huang S and Li Q: LncRNA-PVT1 inhibits ferroptosis through activating STAT3/GPX4 axis to promote osteosarcoma progression. Front Biosci (Landmark Ed) 29: 207, 2024.
39. Sun Z, Li X, Shi Y and Yao Y: LncRNA PVT1 facilitates the growth and metastasis of colorectal cancer by sponging with miR-3619-5p to regulate TRIM29 expression. Cancer Rep (Hoboken) 7: e2085, 2024.
40. Olivero CE, Martinez-Terroba E, Zimmer J, Liao C, Tesfaye E, Hooshdaran N, Schofield JA, Bendor J, Fang D, Simon MD, *et al*: p53 activates the long noncoding RNA Pvt1b to inhibit myc and suppress tumorigenesis. Mol Cell 77: 761-774.e8, 2020.
41. Zhou L, Zhang Q, Cheng J, Shen X, Li J, Chen M, Zhou C and Zhou J: LncRNA SNHG1 upregulates FANCD2 and G6PD to suppress ferroptosis by sponging miR-199a-5p/3p in hepatocellular carcinoma. Drug Discov Ther 17: 248-256, 2023.
42. Xu J, Xu Y, Ye G and Qiu J: LncRNA-SNHG1 promotes paclitaxel resistance of gastric cancer cells through modulating the miR-216b-5p-hexokianse 2 axis. J Chemother 35: 527-538, 2023.
43. Cheng F, Wang L, Yi S and Liu G: Long non-coding RNA SNHG1/microRNA-195-5p/Yes-associated protein axis affects the proliferation and metastasis of gastric cancer via the Hippo signaling pathway. Funct Integr Genomics 22: 1043-1055, 2022.
44. Wang S, Han H, Meng J, Yang W, Lv Y and Wen X: Long non-coding RNA SNHG1 suppresses cell migration and invasion and upregulates SOCS2 in human gastric carcinoma. Biochem Biophys Rep 27: 101052, 2021.
45. He D, Yue Z, Liu L, Fang X, Chen L and Han H: Long noncoding RNA ABHD11-AS1 promote cells proliferation and invasion of colorectal cancer via regulating the miR-1254-WNT11 pathway. J Cell Physiol 234: 12070-12079, 2019.
46. Luo J, Jiang Y, Wu L, Zhuo D, Zhang S, Jiang X, Sun Y and Huang Y: Long non-coding RNA ABHD11-AS1 promotes colorectal cancer progression and invasion through targeting the integrin subunit alpha 5/focal adhesion kinase/phosphoinositide 3 kinase/Akt signaling pathway. Aging (Albany NY) 13: 20179-20191, 2021.
47. Liu Y, Wang LL, Chen S, Zong ZH, Guan X and Zhao Y: LncRNA ABHD11-AS1 promotes the development of endometrial carcinoma by targeting cyclin D1. J Cell Mol Med 22: 3955-3964, 2018.
48. Liu B, Wang W, Sun S, Ding H, Lan L, Li X and Han S: Knockdown of lncRNA ABHD11-AS1 suppresses the tumorigenesis of pancreatic cancer via sponging miR-1231. Onco Targets Ther 13: 11347-11358, 2020.
49. Yang T, Tian S, Zhao J, Pei M, Zhao M and Yang X: LncRNA ABHD11-AS1 activates EGFR signaling to promote cervical cancer progression by preventing FUS-mediated degradation of ABHD11 mRNA. Cell Cycle 22: 2538-2551, 2023.
50. Huang G, Qiu Y, Fan Y and Liu J: METTL3-deficiency suppresses neural apoptosis to induce protective effects in cerebral I/R injury via inhibiting RNA m6A modifications: A pre-clinical and pilot study. Neurochem Res 49: 85-98, 2024.
51. Yang X, Liu X, Nie Y, Zhan F and Zhu B: Oxidative stress and ROS-mediated cellular events in RSV infection: Potential protective roles of antioxidants. Virol J 20: 224, 2023.
52. Fu Y, Ye Y, Zhu G, Xu Y, Sun J, Wu H, Feng F, Wen Z, Jiang S, Li Y and Zhang Q: Resveratrol induces human colorectal cancer cell apoptosis by activating the mitochondrial pathway via increasing reactive oxygen species. Mol Med Rep 23: 170, 2021.
53. Kong F, Xie C, Zhao X, Zong X, Bu L, Zhang B, Tian H and Ma S: Resveratrol regulates PINK1/Parkin-mediated mitophagy via the lncRNA ZFAS1-miR-150-5p-PINK1 axis, and enhances the antitumor activity of paclitaxel against non-small cell lung cancer. Toxicol Res (Camb) 11: 962-974, 2022.
54. Ji Q, Liu X, Fu X, Zhang L, Sui H, Zhou L, Sun J, Cai J, Qin J, Ren J and Li Q: Resveratrol inhibits invasion and metastasis of colorectal cancer cells via MALAT1 mediated Wnt/β-catenin signal pathway. PLoS One 8: e78700, 2013.
55. Cesmeli S, Goker Bagca B, Caglar HO, Ozates NP, Gunduz C and Biray Avci C: Combination of resveratrol and BIBR1532 inhibits proliferation of colon cancer cells by repressing expression of LncRNAs. Med Oncol 39: 12, 2021.
56. Miller CLW, Warner JL and Winston F: Insights into Spt6: A histone chaperone that functions in transcription, DNA replication, and genome stability. Trends Genet 39: 858-872, 2023.
57. Nojima T and Proudfoot NJ: Mechanisms of lncRNA biogenesis as revealed by nascent transcriptomics. Nat Rev Mol Cell Biol 23: 389-406, 2022.
58. Shehzada S, Noto T, Saksouk J and Mochizuki K: A SUMO E3 ligase promotes long non-coding RNA transcription to regulate small RNA-directed DNA elimination. Elife 13: e95337, 2024.
59. Diao C, Guo P, Yang W, Sun Y, Liao Y, Yan Y, Zhao A, Cai X, Hao J, Hu S, *et al*: SPT6 recruits SND1 to co-activate human telomerase reverse transcriptase to promote colon cancer progression. Mol Oncol 15: 1180-1202, 2021.
60. No authors listed: Retraction: lncRNA ABHD11-AS1, regulated by the EGFR pathway, contributes to the ovarian cancer tumorigenesis by epigenetically suppressing TIMP2. Cancer Med 13: e7098, 2024.
61. Lu H, Zhu C, Chen Y, Ruan Y, Fan L, Chen Q and Wei Q: LncRNA ABHD11-AS1 promotes tumor progression in papillary thyroid carcinoma by regulating EPS15L1/EGFR signaling pathway. Clin Transl Oncol 24: 1124-1133, 2022.
62. Richiardone E, Al Roumi R, Lardinois F, Giolito MV, Ambroise J, Boidot R, Drotleff B, Ghesquière B, Bellahcène A, Bardelli A, *et al*: MCT1-dependent lactate recycling is a metabolic vulnerability in colorectal cancer cells upon acquired resistance to anti-EGFR targeted therapy. Cancer Lett 598: 217091, 2024.